2014 IEEE International Conference on Robotics & Automation (ICRA)
Hong Kong Convention and Exhibition Center
May 31 - June 7, 2014. Hong Kong, China

Development of a Coupled Tendon-Driven 3D Multi-joint Manipulator

Atsushi Horigome[1], Hiroya Yamada[2], Gen Endo[1], Shin Sen[3], Shigeo Hirose[4] and Edwardo F. Fukushima[1]

***Abstract*— Very long-reach snake-like robotic arms in the range of 14 meters are expected to be used in decommissioning work inside nuclear reactor containers. We developed a tendon-driven system which has the advantage of placing electronic devices protected in the arm's base part which stays out of the reactor container, and only few expensive highly radiation hardened sensors and tools are mounted in the arm tip. Generation of large joint torque is necessary to realize such a very long arm. We applied the concept of coupled tendon-driven mechanism formerly used to generate restricted two dimensional motions, and extended its concept by proposing a new joint arrangement which makes possible three dimensional motions in a large workspace. Mechanical design, compact storage method and derivation of the arm motion control are detailed. Moreover, we built a preliminary mechanical prototype called "Mini 3D CT-Arm", and the experimental results demonstrated the validity of the newly proposed concept.**

I. INTRODUCTION

A tendon-driven multi-joint manipulator whose actuators are installed in the base unit has many advantages compared with a manipulator whose actuators are equipped in its joints. For example, since it does not have heavy actuators in its arm, it is possible to reduce the total weight of the arm, and consequently make actuators small and an arm slim. In addition, since it does not have electronic components in its arm, it can work in extreme environment, underwater or under high radiation. In this paper, taking advantage of the above, we aim at development of the tendon-driven multi-joint manipulator, which can access to narrow space, with a length of over 10 meters required in an actual disaster site.

Many tendon-driven robot arms are developed until now. One of the conventional methods to construct a redundant multi-joint arm is to radially arrange the wires and make a bending motion by pulling and relaxing the wires [1] [2] [3]. These arms can be slim and have multi-degree-of-freedom (DOF). For example, Fig. 1(a) shows "Snake Arm Robot" (OC Robotics Corp.) [4] [5]. It is driven by many wires from the base unit, and three wires attached at equal intervals drive one joint. However, since each driving wire goes through many arm segments and generates sliding motion when the wire is pulled, the frictions between the wire and structural parts increase when the total length of the arm increase and/or the arm makes a very sharp bending. Thus, it might be difficult for this method to develop a very long and slim arm whose length is over 10 meters.

In this paper, we will focus on the robot arm which has rigid links driven by wires and pulleys in order to develop a longer and slimmer arm than conventional robot arm. Since all driving wires are transmitted via passive rotating pulleys with sufficiently large radius, the frictions between the wires and structural parts are greatly reduced thanks to the rolling contact of passive pulleys. In our previous work [6], a coupled tendon-driven multi-joint long manipulator "CT-Arm I", as shown in Fig. 1(b), can generate large torque in the proximal joint without using large motors or thick wires by involving the tension of each wire. However, joint axes of CT-Arm I in the arm were all in the pitch direction and therefore the redundant dexterous manipulation was limited only in 2-dimension, although there was a swivel joint at the base to make it 3-dimensional polar coordinate motion. In this paper, in order to enhance the accessibility and dexterity in narrow and confined space, we develop a coupled tendon-driven 3D multi-joint manipulator "3D CT-Arm" which can move and work in 3-dimension by introducing multiple yaw joints in the distal arm segments.

The organization of this paper is as follows. In section II, we design 3D CT-Arm for a decommissioning work of Fukushima Daiichi nuclear power plant. In section III, we describe the relation between the winding length of the tendon and each joint angle and the one between the wire tension and the joint torque for control. In section IV, we describe the development of preliminary prototype model and the basic experiment of control. In section V, a summary is given.

(a) MOD Snake-Arm (OC Robotics) (courtesy of OC Robotics)

(b) CT-Arm I (TITech)

Fig. 1. Examples of tendon-driven manipulators

[1]A.Horigome, G.Endo and E.F.Fukushima are with the Department of Mechano-Aerospace Engineering, Tokyo Institute of Technology, 2-12-1 Ookayama, Meguroku, Tokyo, 152-8552, Japan horigome.a.aa@m.titech.ac.jp, gendo,fukushima@mes.titech.ac.jp

[2]H.Yamada is with Global Edge Institute, Tokyo Institute of Technology, 2-12-1 Ookayama, Meguroku, Tokyo, 152-8552, Japan yamada@robotics.mes.titech.ac.jp

[3]S.Sen is with the Department of Precision Engineering, The University of Tokyo, 7-3-1 Hongo, Bunkyoku, Tokyo, 113-0033, Japan shin@bmpe.t.u-tokyo.ac.jp

[4]S.Hirose is with the HiBot Corp, 2-18-3 Shimomeguro, Meguroku, Tokyo, 152-0064, Japan hirose@robotics.mes.titech.ac.jp

II. Mechanical Design of 3D CT-Arm

A. Target specification

We consider 3D CT-Arm expanding its arm in the reactor container of Fukushima Daiichi nuclear power plant and investigating it, as shown in Fig. 2. In the press release from Tokyo Electric Power Company (TEPCO) about a mid- to long-term plan for the removal of atomic fuel debris, TEPCO plans to investigate the bottom part of the primary containment vessel (PCV) to find cooling water leakage. After boring a hole to PCV, a camera and various measurement devices will be inserted and inspect PCV inside [7]. To deliver a camera and the other devices, a long and slim arm is really suitable. We assume that the required total length of the arm is 14 m and the diameter of the arm is 0.3 m, because the diameters of the PCV sphere and inspection hole in the actual site are 18 m and 0.3 m, respectively [8] [9]. In addition, the arm should be stored small to be carried to a workspace. From the above, we decide the specification of 3D CT-Arm as shown in table I. The stowed size is estimated by the size of double doors (single door size is shown in [10]).

Here, we estimate the torque required for the joint in the most proximal joint (1st joint) in order to support an arm horizontally, the tension of the wire which drives the 1st joint and the diameter of the wire using a conventional design. We show a geometrical model in Fig. 3. We assume the weight (M) and the length (L) of the arm and the diameter (D) of a pulley as $M = 100\,\mathrm{kg}$, $L = 14\,\mathrm{m}$ and $D = 0.3\,\mathrm{m}$. In this case, the torque (T) required for the 1st joint and the tension (F) of the wire are calculated as

$$T = \frac{MgL}{2} = 6860\,\mathrm{Nm} \quad \text{and} \quad F = \frac{T}{D/2} = 45.7\,\mathrm{kN}. \quad (1)$$

Now, we calculate the diameter of a wire in order to exert the tension F. If we select a standard stainless wire with safe factor of 2.0, the diameter of wire d should be larger than 14 mm. In order not to decrease strength of the wire by bending, D/d should be kept larger than 15. Thus, the driving pulley to pull the wire should be larger than 210 mm, which is not compact. Moreover, the torque T is really huge. To the best of our investigation, a reduction unit which can output such a high torque is RV reducer (RV-500C: NABTESCO). However, its diameter and weight are 520 mm and 160 kg, respectively [11]. These results clearly show that conventional design can not satisfy the requirement in size. To solve the problem, we introduce the principle of a coupled tendon driven mechanism adopted in CT-Arm I, which can generate large torque in the 1st joint with small multiple actuators.

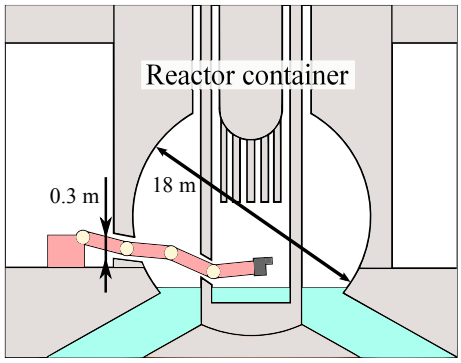

Fig. 2. The concept of 3D CT-Arm in Fukushima Daiichi nuclear power plant

TABLE I
Target specification of a robot arm

Arm length	14 m
Arm diameter	0.3 m
A size of storage configuration	Less than 2 m in width, 2 m in length and 2 m in height

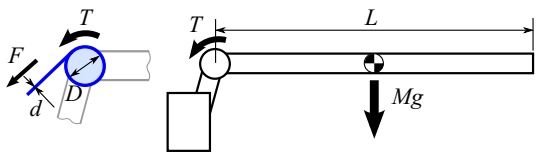

Fig. 3. A calculate model of the torque in the 1st joint

B. A Coupled Tendon-Driven Mechanism of CT-Arm I

We show the principle of a large torque generation on the proximal joint by a coupled tendon-driven mechanism applied to CT-Arm I in Fig. 4. The wire which drives each joint is wound around the fixed pulley (link driving pulley) of the distal joint. The wire is wound around passive pulleys (transfer pulleys) from the proximal joint to the distal joint, and the wires are pulled by actuators mounted on the base structure. Therefore, tension of the wire can generate torques in all joints around which the wire is wound, and three wires' tension participate in torque generation for the proximal joint, which usually requires large torque to sustain the arm. For example, in Fig. 4, if we pull three wires with force F which drive each joint upward, torques generated in each joint are $T(= rF), 2T$ and $3T$, respectively where r is the radius of the pulley. Using this principle, we can generate large torques on the proximal joints by coupling multiple actuators' torque instead of using large actuators[6]. In 3D CT-Arm, if wire is *Zylon*, light and high strength fiber, the

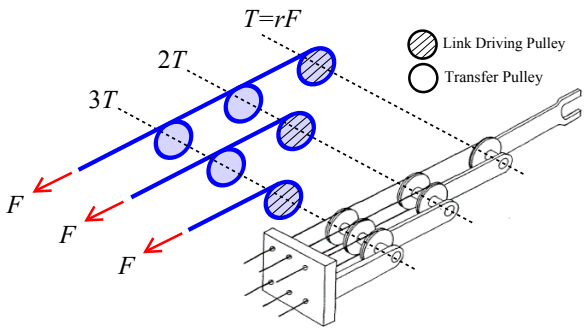

Fig. 4. The principle of CT-Arm I

diameter of wire should be only 2.5 mm, and a reduction unit can be HarmonicDrive (CSF-45-120: Harmonic Drive Systems) whose diameter and weight are 155 mm and 2.3 kg respectively [12].

C. Proposal of a New Joint Arrangement for Three Dimensional Movements

Although CT-Arm I has a swivel degree of freedom in the base joint, the coupled tendon-driven arm has only pitch axes. Thus it is very difficult to access a very narrow and confined space. Therefore, in this paper, we propose to install yaw axes in addition to pitch axes in the distal segments of the arm. Figure 5 a new pulley arrangement achieving both pitch and yaw movements by coupled tendon-driven mechanism. By pulling one of the two wires which drives the yaw axis, the yaw joint can turn right and left shown in Fig. 5(a) and (b). Since two wires are wound around via pulleys of the pitch axis, if we pull both wires, torque can be generated in the pitch axis and the arm can go up as shown in Fig. 5(c). By this means, it is possible for the wire tensions which are used to move the yaw joints to generate torque in the direction which raises a pitch axis. As a result, we can generate a large torque in the proximal joint by coupled tendon-driving mechanism using multiple tendon traction forces.

We design 3D CT-Arm having 18 DOF as shown in Fig. 6 using the above-mentioned principle. The length of arm is 14 meter and the arm has 12 pitch axes and 6 yaw axes. For proximal joints, there are only pitch axes because main purpose of the proximal joints is to extend the arm. On the other hand for distal joints, there are pitch and yaw axes alternately in order to avoid obstacles in a narrow and confined space.

D. Containment Configuration

When a long robot arm works in extreme environment, it is very important to compact containment for the ease of deployment in the site. In this section, we describe containment and expanded configurations of the arm shown in Fig. 7. It is possible to twist and coil around a square drum

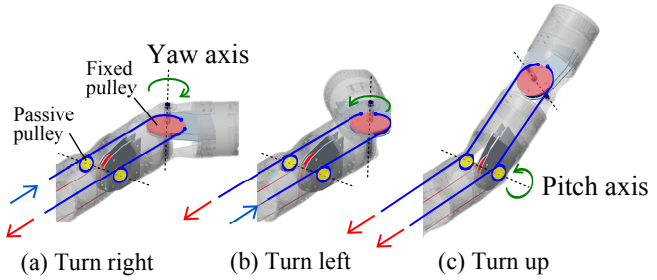

Fig. 5. 3D motion of 3D CT-Arm

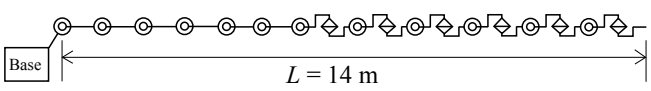

Fig. 6. The concept of 3D CT-Arm

if the distance of the pitch joints are identical. However, if all pitch axes are parallel to each other, we can not make multiple turns due to the collision shown in Fig. 8(a). However, if the direction of each pitch axis is shifted in the roll direction, it can be twisted any number of rounds as shown in Fig. 8(b). We derive the phase difference between the kth and the $(k+1)$th pitch axis (ϕ_k) in the roll direction, the inclination of the whole arm denoted as ψ and the joint angle of the kth pitch axis in the containment configuration (θ_k).

Figure 9 shows the kinematic model of calculation. We define the arm length as L and the interval of twist as d. In the expanded configuration, the standard position of the arm is along to the x axis, and its pitch axes are orthogonal to the x axis. From this configuration, the root structure is rotated $(-\psi)$ around the y axis and kth pitch axis is rotated θ_k. In this case, the length of one side of the square prism

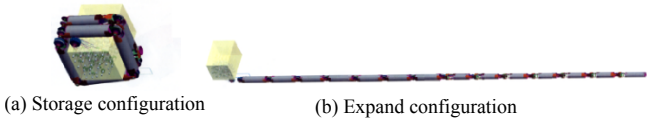

Fig. 7. The concept of storage motion

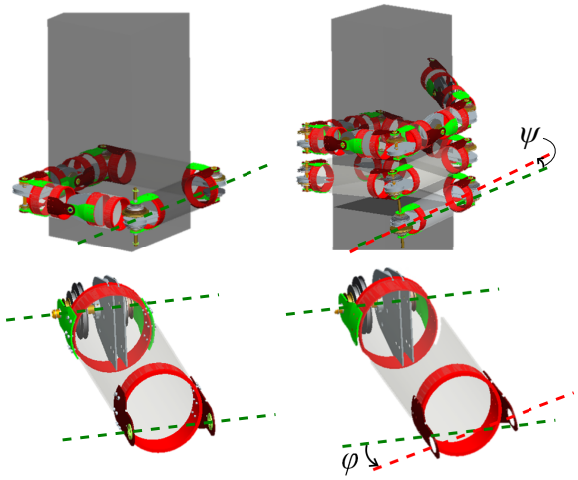

Fig. 8. The principle of storaging

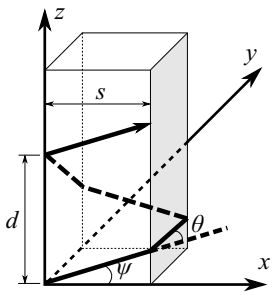

Fig. 9. The calculate model

(s) and ψ are expressed as

$$s = \sqrt{l^2 - \left(\frac{d}{4}\right)^2} \quad \text{and} \quad \psi = \sin^{-1}\left(\frac{d}{4l}\right). \tag{2}$$

Next, we derive the phase difference between the 1st and the 2nd pitch axis ϕ_1, and the angle of the 1st pitch axis θ_1 in containment configuration. The vector of each link in the standard position $\hat{\boldsymbol{l}}$ and the vector of the 2nd link in the containment configuration $\boldsymbol{l_2}$ are expressed as

$$\hat{\boldsymbol{l}} = [\, l \; 0 \; 0 \,]^T \quad \text{and} \quad \boldsymbol{l_2} = \boldsymbol{E}^{j(-\psi)}\boldsymbol{E}^{i(\phi_1)}\boldsymbol{E}^{k(\theta_1)}(\hat{\boldsymbol{l}}). \tag{3}$$

by using rotation matrices of each xyz axis $\boldsymbol{E}^i, \boldsymbol{E}^j and \boldsymbol{E}^k$. Here, $\boldsymbol{l_2}$ is the same as the vector that $\boldsymbol{l_1}(= \boldsymbol{E}^{j(-\psi)}(\hat{\boldsymbol{l}}))$ is rotated $\pi/2$ in the z axis. Therefore, we obtain

$$\boldsymbol{E}^{j(-\psi)}\boldsymbol{E}^{i(\phi_1)}\boldsymbol{E}^{k(\theta_1)}(\hat{\boldsymbol{l}}) = \boldsymbol{E}^{k(\pi/2)}\boldsymbol{E}^{j(-\psi)}(\hat{\boldsymbol{l}}). \tag{4}$$

From (4), we can get ϕ_1 and θ_1 as

$$\phi_1 = \tan^{-1}(\sin\psi) \quad \text{and} \quad \theta_1 = \cos^{-1}(\sin^2\psi). \tag{5}$$

If we think the same way, we can get ϕ_k and θ_k as

$$\phi_k = \begin{cases} \tan^{-1}(\sin\psi) & (k=1) \\ 2\tan^{-1}(\sin\psi) & (k \geq 2) \end{cases} \tag{6}$$

$$\text{and} \quad \theta_k = \cos^{-1}(\sin^2\psi). \tag{7}$$

From the above, the mechanical design parameters required in the containment configuration are obtained.

III. Joint Control Strategy

In the case of 3D CT-Arm, the wire which drives one joint also affects torque generations in the other joints. In this section, for the control of 3D CT-Arm, we describe the position control by measuring the angle of each joint and controlling the winding length of the tendon. We also discuss the tension control by measuring the tension of each wire and controlling torque of each joint.

A. The Relation between the Winding Length of the Tendon and Each Joint Angle

When the wire drives the ith joint, the winding length of the tendon is calculated from the change of each joint angle from the 1st joint to the ith joint because the wire is wound around the link driving pulley of the ith joint via the transfer pulleys of each joint from the 1st joint to the $(i-1)$th joint. We define θ_j as the relative angle to the jth link of the $(j-1)$th link and $\Delta\theta_j$ as the difference between measured and desired value of θ_j. Here, $S_i^{\pm}$, the winding length (which drives the ith joint), is expressed as

$$S_i^{\pm} = \sum_{j=1}^{i} \delta_{ij}^{\pm} r_{ij} \Delta\theta_j. \tag{8}$$

When θ_i becomes large by the wire being wound, the winding length is expressed as S_i^+. S_i^- is the winding length of opposite wire. $\delta_{ij}^{\pm}$ is the value of +1 or -1, determined by the winding direction of the ith joint driving tendon around the jth joint whose pulley radius is r_{ij}.

B. The Relation between the Wire Tension and the Joint Torque

The ith joint torque is generated by tension of wires which are wound around link driving pulley and transfer pulleys of the ith joint. Wires which drive joints from the $(i+1)$th joint to the Nth joint are wound around transfer pulleys of ith joint. Therefore, if the tension of the wire which drives the jth joint is $F_j^{\pm}$, the torque generated in the ith joint is expressed as

$$T_i = \sum_{j=i}^{N} \delta_{ji}^{\pm} r_{ji} F_j^{\pm}\,, \tag{9}$$

where N is the number of joints. F_j^+ and F_j^- are the each tension of two wires wound around the link driving pulley of the jth joint. The definition of $\delta_j^{\pm} i$ is the same as Eqn.(8).

IV. Development of Preliminary Prototype Model Mini 3D CT-Arm and its Control Experiment

We developed a preliminary experiment model "Mini 3D CT-Arm" which had 6 joints before the developing the full size 3D CT-Arm. In Mini 3D CT-Arm, we aim at verifying the following matters.

- Whether the coupled tendon-driven arm which has both yaw axes and pitch axes can move.
- Whether the arm does not move in vibration because of many coupled tendon-driven mechanisms.
- Whether the elasticity of a new material wire introduced for the weight saving doesn't cause problems.

In this section, we describe the design of Mini 3D CT-Arm and its basic experiment.

A. Design of Mini 3D CT-Arm

Figure 10 shows the overview of Mini 3D CT-Arm. We arranged four pitch axes so that the motion of proximal links following the first distal link can be performed. In addition, we arranged two yaw axes in the two distal links so that we confirm a coupled tendon-driving effect of yaw axes which is newly installed in 3D CT-Arm to enlarge the arm workspace. The diameter of the arm is 0.15 m and the length is 2.4 m. The base unit has motors, motor drivers and microcomputers. We use wires (HAYAMI INDUSTRY CO.: DY-20ZL, $D = 2.0\,\mathrm{mm}$) , whose cores are *Zylon*[1] which are made of PBO fiber, one of the lightest and highest strength fiber. The core fibers are covered with *Dyneema* sleave. The each joint of arm has a single link driving pulley (black) and several transmission pulleys (white) on the same axis. Pulleys are made of polyacetal plastic for a weight saving. The main structural parts of the arm are made of acrylic plastic and aluminum alloy.

We show the structure and arrangement of joints, pulleys and wires in Fig. 11. We define the joint number from

[1]Zylon is not suitable for long term operation for several months in high humidity environment because of its hydrolytic degradation property. We need to careful investigation about environmental condition and appropriate wire materials for real application.

proximal joint to distal joint. Each joint is driven by two motors and two wires attached in the same way as 3D CT-Arm. The wire is wound around the link driving pulley via the transfer pulleys of each proximal joint. Torque can be generated on the transfer pulleys of each joint by tension of wires.

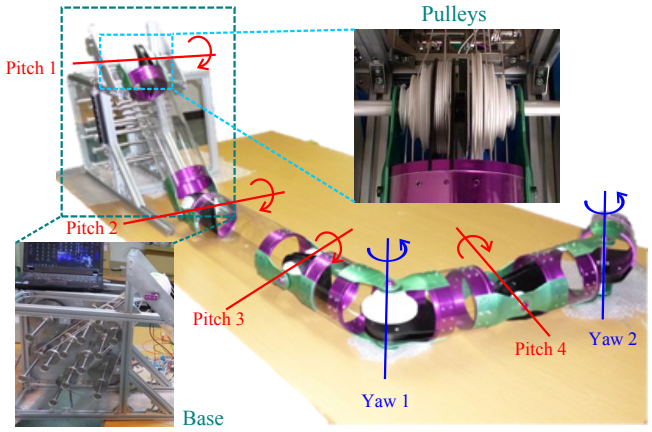

Fig. 10. Mini 3D CT-Arm

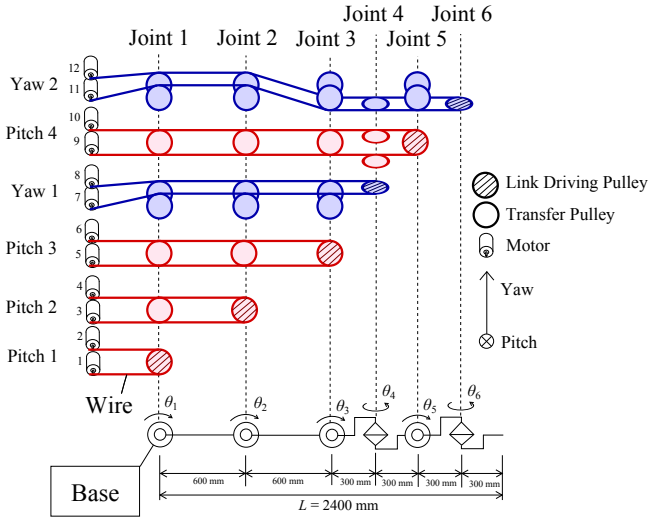

Fig. 11. The construction of joints, pulleys and wires of Mini 3D CT-Arm

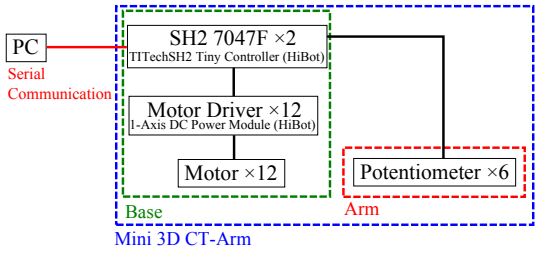

Fig. 12. Control System

B. Configuration of Control System

We show the configuration of the control system in Fig. 12. We can operate by measuring angles of each joint with potentiometers. A tension sensor is not equipped in this model. The microcomputers are two *TITechSH2 Tiny Controller* (Hibot Corp.), and the motor drivers are twelve *1-Axis DC Power Module* (Hibot Corp.). Potentiometers are installed to each joint of arm. Motors, motor drivers and microcomputers are mounted on the base unit. We calculate each joint angle with PC and control SH2 by serial communication. Two SH2 read the value of potentiometers and drive motors.

Table II shows the installed actuators. Motor number i specifies the installed motor i in Fig. 11. Small output motors are used for pitch down or yaw axes driving and large output motors are used for pitching up motion.

C. Control Experiment

In control experiment, we specified a target trajectory to be followed by the arm and controlled positions of joint angles with (8). We controlled each motor with PI control by considering the winding length ($S_i^{\pm}$). In addition, we did not drive the motors at $S_i^{\pm} < 0$ and made the motors back-driven with the tension of wires in order not to slack. However, since some motors did not have sufficient backdrivability, we drove these motors in 20% of the value calculated in (8) at $S_i^{\pm} < 0$.

Figure 13 shows the control experiment. From the first position (a), each joint moved along with the curve we set up and the arm became the last position (d). After that, the arm followed the same locus and returned to the first position. We experimented repeatedly and obtained the time course of the desired and measured joint angles shown in Fig. 14. We can confirm that most of the joints track desired angle with, although there are some delays, sufficient accuracy. The tracking of the 6th joint angle is inferior to other joints because the motors' torque of the 6th joint is smaller than others. We can improve it by introducing higher reduction ratio. In the tracking of the other joints, first, the 5th joint angle has relativery large errors for 40 s to 55 s and 95 s to 110 s. This is because it takes time to wind the slack wire which is sent out to put the link down in the previous step(20 s to 40 s or 75 s to 95 s). At 44 s, the improvement of the 5th joint angle is triggered by the 4th joint. The 4th joint angle has relatively large errors at 44 s and 117 s. This is because the 4th joint, yaw axis, moves easily by gravity if its wires are slack. At 44 s, the wires which are fixed

TABLE II
DETAILS OF MOTORS

Maker	Nippo Denki	SHAYANG YE INDUSTRIAL	maxon motor	maxon motor
Rated voltage	30 V	24 V	48 V	24 V
Output	90 W	48 W	150 W	150 W
Reduction ratio	31.5	43	230	81.1
Rated torque	0.49 Nm	1.6 Nm	23 Nm	9.4 Nm
Motor number	1,3,5,9,11,12	7,8,10	2	4,6

the 4th joint start send out because the 3rd joint starts up its angle. This is the same at 117 s. These errors can be reduced by being equipped with force sensors and maintaining wire tension.

From the result, we confirmed that the coupled tendon-driven arm which has both yaw axes and pitch axes can move without vibration by using a new material wire.

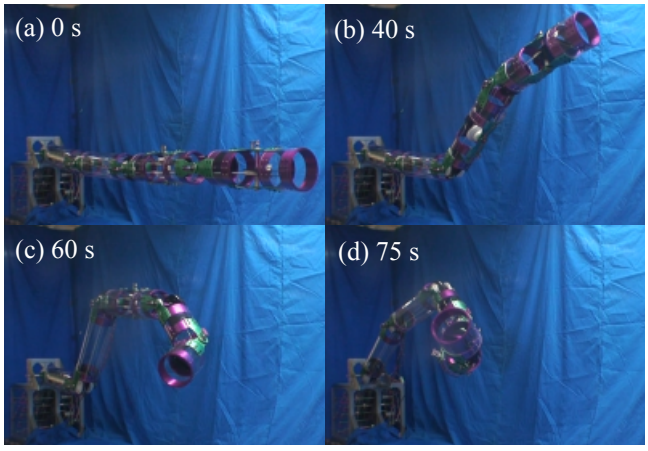

Fig. 13. Experiment of Mini 3D CT-Arm operation

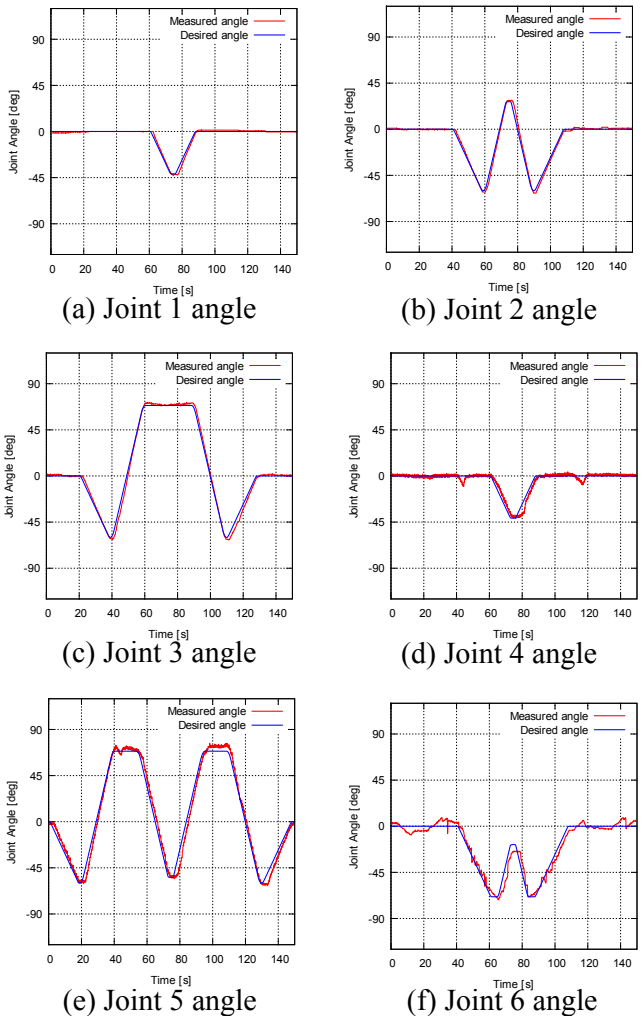

Fig. 14. The time history of each joint angle

V. CONCLUSIONS

We proposed a coupled tendon-driven 3D multi-joint manipulator 3D CT-Arm for extreme environment task such as a decommissioning of a nuclear power plant. 3D CT-Arm has the pitch and yaw degrees of freedom and can potentially work in the narrow confined space which is very difficult to access. We derived the containment configuration winding around a square prism for carrying arm and obtain the design parameters to achieve the configurations. In 3D CT-Arm operation, we clarified the relation between the winding length of the tendon and the angle of each joint as well as the relation between the wire tension and the joint torque. Finally, we developed the preliminary experiment model Mini 3D CT-Arm and demonstrated the motion in 3D space with position feed-back control. We confirmed that the measured angle followed the desired angle with sufficient accuracy.

In future work, we plan to install tension sensors and achieve a feed-forward control to cancel the gravitational force. Comparison between force feed-forward control and position feedback control may contribute to develop full-sized 3D CT-Arm.

ACKNOWLEDGMENT

A part of this research received support of the JSPS Grants-in-Aid for Scientific Research (25420214).

REFERENCES

[1] Shigeo Hirose, Takashi Kado, Yoji Umetani; Tensor Actuated Elastic Manipulator, Proc. 6th IFToMM World Congress, 2, pp.978-981 (1983)

[2] G. Robinson, J. B. C. Davies, "Continuum Robots - A State of the Art", ICRA, pp. 2849-2854 (1999)

[3] D. B. Camarillo, C. R. Carlson, J. K. Salisbury; Configuration Tracking for Continuum Manipulators With Coupled Tendon Drive, IEEE TRANSACTIONS ON ROBOTICS, vol.25, No.4, pp.798-808 (2009)

[4] R. O. Buckingham, A. C. Graham, "Dexterous manipulators for nuclear inspection and maintenance - case study", CARPI (2010)

[5] OC Robotics (http://www.ocrobotics.com/)

[6] S. Hirose, S. Ma, "Coupled Tendon-Driven multi-join Manipulator", in Proc. ICRA, pp. 1268-1275 (1991)

[7] TEPCO: a mid- to long-term plan for the removal of atomic fuel debris(http://www.nsr.go.jp/committee/yuushikisya/tokutei_kanshi/data/0006_04.pdf)(in Japanese)

[8] TEPCO: Specification of Fukushima Daiichi Nuclear Power Plant(http://www.tepco.co.jp/nu/f1-np/intro/outline/outline-j.html)(in Japanese)

[9] TEPCO: Press Release on Feb.14th (2013)(http://www.tepco.co.jp/nu/fukushima-np/handouts/2013/images/handouts_130214_02-j.pdf)(in Japanese)

[10] Field Exploration in the Torus Room(http://www.meti.go.jp/earthquake/nuclear/pdf/120328_02aa.pdf) (in Japanese)

[11] NABTESCO RV-C Series (http://www.nabtescomotioncontrol.com/pdfs/RV-Cseries.pdf)

[12] General Catalog of HarmonicDrive pp. 40-41 (http://hds-tech.jp/pdf/hd01_en.pdf)